AIMS Materials Science, 3(2): 634-644.
DOI: 10.3934/matersci.2016.2.634
Received: 07 March 2016
Accepted: 24 May 2016
Published: 26 May 2016

http://www.aimspress.com/journal/Materials

Research article

Microstructural features associated with the effect of temperature on the dimensional stability of an automotive Al-A319 alloy

Hugo F. Lopez

Materials Science and Engineering Department, University of Wisconsin-Milwaukee, 3200 N. Cramer Street, Milwaukee WI 53211, USA; Email: hlopez@uwm.edu; Tel: 414-229-6005.

Abstract: In this work an automotive Al-A319 was given a solid solution heat treatment (T4) at 753 K (480 °C) for 4.5 hours and an ageing treatment (T7) at 513 K (240 °C) for various times up to 3.0 h. The alloy in the T4 condition was dilatometrically tested at various temperatures in order to measure its relative dimensional changes. It was found that the dimensional changes are due to both, alloy thermal expansion and nucleation and growth of second phases. In addition, in the T7 condition the alloy strength and ductility were determined as a function of ageing times. Ageing promoted alloy strength but at the expenses of a rather poor alloy ductility (down to 1%). Apparently, Cu rich intermetallic phases and regions provided a brittle path for fracturing. In particular, microstructural characterization using high resolution transmission electron microscopy indicated that not all the Cu in the matrix was dissolved during the T4 treatment. Hence, after ageing (T7) these Cu-rich regions seemed to coarsen into spherical particles.

Keywords: Al-Si-Cu-Mg alloys; dimensional stability; solid solution treatment; ageing; mechanical strength

1. Introduction

The demand for energy efficient vehicles has led to an increasing use of aluminum alloys in manufacturing various engine components including engine blocks. In particular, the Al-A319 automotive alloy has been widely employed due to its high temperature strength. The alloy possesses elevated strength and hardness which do not fall rapidly with temperature [1–4]. Nevertheless, this alloy is rather brittle as the ductility is typically between 1–3%. The alloy properties can be attributed to the large number of secondary phases that are precipitated upon casting, including large

intermetallic compounds. A large number of these intermetallic phases are Fe-containing brittle compounds as the alloy contains iron as a common impurity. Typical alloy microstructures are coarse dendrites surrounded by silicon particles and complex intermetallic phases which give rise to the classical "Chinese scripture" morphology. In addition, the alloy contains Cu and Mg as alloying elements which give rise to two eutectics upon solidification, θ (Cu_2Al) + α at 821 K (548 °C) and a low temperature eutectic α + β (Al_3Mg_2) at 723 K (450 °C), both of them brittle. Most of the alloying elements particularly Fe give rise to brittle coarse intermetallics [5,6].

In order to avoid the effects of an inhomogeneous distribution of impurities including alloying elements the alloy is typically solubilized (T4) and solubilized followed by quenching and ageing (T7). However, under these conditions the alloy dimensional stability undergoes changes. In turn, geometrical distortions and/or failure can be experienced in these alloy castings when proper procedures are not incorporated to take into account the effects related to these dimensional changes. In addition, Al-A319 automotive alloys are prone to undergo temperature variations as they are used for casting engine blocks. Under these conditions the alloy experiences thermal expansion and second phase precipitation, both of which can modify the casting alloy dimensions and properties.

In order to avoid possible negative effects of dimensional instabilities on the mechanical alloy integrity, in this work, typical T4 and T7 heat treatments are investigated using dilatometry and tensile testing. This is followed by microstructural characterization including transmission electron microscopy (TEM).

2. Materials and Method

A commercial Al-A319 alloy was prepared by melting in an induction furnace; the liquid metal was degasified and modified with Al-10% Sr alloy. This was followed by casting into bar shaped molds of 2.5 cm × 5.0 cm × 10.0 cm. The resultant alloy chemical composition is given in Table 1. From this alloy cylindrical bars 0.5 cm by 5.0 cm were machined for dilatometric determinations. In order to establish the thermal expansion effects excluding precipitation reactions, blank dilatometric samples of pure aluminum (99.999%) were tested. In addition, tensile bars were made for tensile testing. From the as-cast and heat treated bars, cylindrical tensile specimens of 9 mm in diameter by 80 mm in length were machined according to the ASTM standards E21-921998 and B557-02. Tensile testing was carried out on an MTS 810 machine at a strain rate of $10^{-4}\ s^{-1}$. Four samples were tested at each test temperature in order to obtain reliable tensile results. T4 heat conditions were obtained by heat treating the as-cast specimens at 753 K for 4.5 hours and cooling in forced air. In addition, T7 samples were produced by aging the T4 specimens at 513 K for various times (up to 2.6 hours) and air cooling to room temperature.

Table 1. Chemical composition of the A319 castings (wt.%).

Si	Fe	Cu	Mn	Mg	Sr	Cr	Ni	Pb	Al
8.6	0.5	3.8	0.3	0.36	0.012	0.05	0.023	0.015	Bal

The alloys were metallographically prepared for optical microscopy. Further microstructural characterization of the exhibited phases and fracture surfaces was carried out using a scanning

electron microscope (SEM) FEI Quanta 200. This was followed by cutting and preparing thin foils for transmission electron microscopy (TEM). The thin foils were obtained by jet polishing in a solution of 30% acetic acid, 20% orthophosphoric acid, 40% of water and 10% of nitric acid and then by ion milling in an Argon atmosphere.

3. Results and Discussion

Figure 1 shows the as-cast microstructure and the effect of the solid solution T4 heat treatment (HT) on the morphology and size of the Si particles. At the solid solution temperature, thermally activated processes such as Sr diffusion in the neighborhood of Si eutectic combined with a reduction in interfacial energy become actively involved. Consequently, it can be observed that the solid solution treatment promotes Si coarsening and coalescence, as well as the removal of sharp Si particle edges.

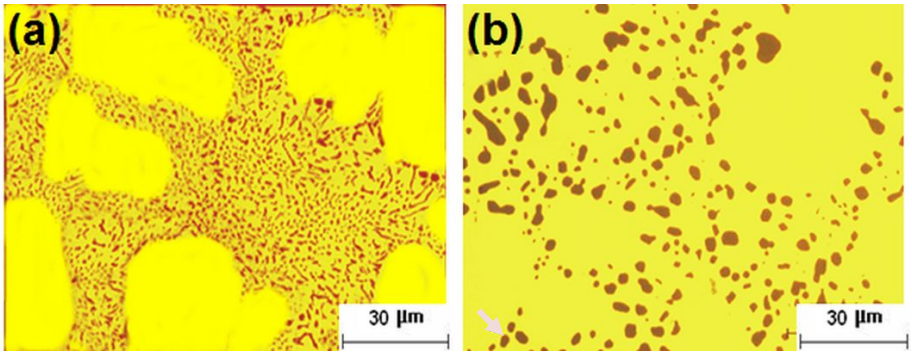

Figure 1. Effect of solid solution HT (T4) on the size and morphology of Si particles in the A319 Al alloy. (a) As-cast alloy and (b) after solid solution at 753 K (480 ^{o}C) for 4.5 hours.

The Al A319 alloys are known for the elevated amounts of coarse brittle intermetallic phases with a large number of them containing Fe [7]. In turn, the exhibited alloy microstructure is known as the "Chinese scripture." In addition, the alloy possesses relatively high temperature strength partly due to the intermetallic phases present. Nevertheless, the alloy ductility and toughness is rather poor, particularly in the as-cast condition. This becomes a serious limitation for potential alloy applications. Figure 2a shows Al-Cu intermetallics and the typical Chinese scripture (Figure 2b).

In the as-cast condition the alloy properties are non-homogeneous due to appreciable solute segregation. Hence, in order to eliminate the segregated microstructure, a solid solution treatment (T4) is typically implemented. Nevertheless, the alloy strength might not be optimal and further processing is implemented such as ageing at high temperatures for various times (T7 heat treatments) depending on the desirable alloy strength.

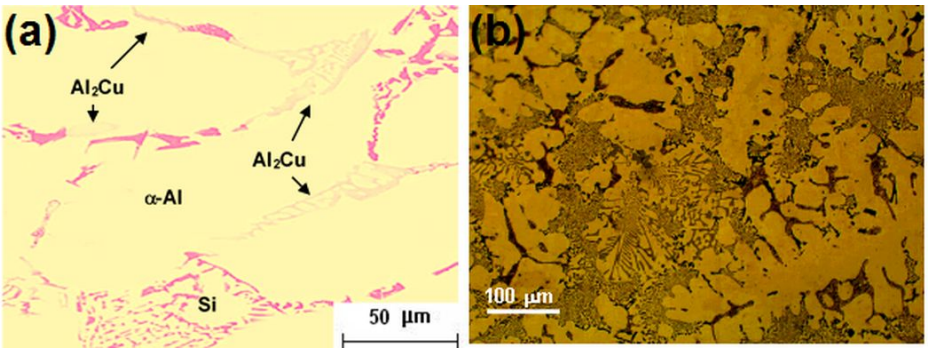

Figure 2. Optical micrographs showing (a) Cu-intermetallics and (b)chinese scripture containing needle shaped Fe-intermetallics in the as-cast A319 Al alloy condition.

In the T7 condition the alloy is prone to develop metastable precipitates when exposed to temperatures just above room temperature [8]. The series of precipitation reactions which give rise to metastable phases all the way to the equilibrium phase (θ) are well known [9]. In the particular case of Al-Cu alloys containing up to 4.5% Cu the precipitation sequence as a function of time at the ageing temperatures is

$$\alpha_{SS} \rightarrow \alpha_1 + \text{GP zones} \rightarrow \alpha_2 + \theta'' \rightarrow \alpha_3 + \theta' \rightarrow \alpha_4 + \theta$$

where α_i is the Al-matrix structure with i equal to 1to 4 describing the amount of Cu remaining in solid solution with the transformation times. The sequence and length of each of the transformations for the metastable phases might change depending on temperature [7,8]. Also, alloying additions might promote the development of other metastable phases and precipitation sequences [9]. Assuming that the main metastable phases developed correspond to the aforementioned phases, the formation of each of these phases is concomitant with a net volume increase. Table 2 gives the volume increases accompanying each of these metastable phases.

Table 2. Volume increases associated with the formation of second phases in Al-Cu alloys [10].

Precipitating phase	(% Cu) in phase	V_{Cu} (cm^3/g)
θ	54.2	0.2299
θ′	54.2	0.2427
θ′′	44.0	0.2611

Notice in particular that application of the A319 Al alloy in the as-cast or solid solution condition is expected to undergo dimensional changes when operating at high temperatures. These dimensional changes can be detrimental particularly if operating conditions locally lead to conditions which exceed the alloy strength or ductility. In order to avoid the potential effects of uncontrolled dimensional stability, T7 heat treatments can provide the required alloy dimensional stability through the development of the metastable phases and through the concomitant improvement in alloy strength.

3.1. Dilatometry

A determination of the extent of dimensional changes and the effect of T4 and T7 heat treatments can be followed by dilatometric means. Figure 3a shows the dimensional changes associated with the alloy thermal expansion and intrinsic phase precipitation reactions at various temperatures in the Al-A319 alloy. In particular, notice that up to one hour or so depending on temperature, might be needed to reach a stable dimensional condition. Figure 3b shows the dimensional changes exhibited at 513 K (240 °C). In this case, a blank dilatometric bar (pure Al) is used to disclose the contribution of thermal expansion from the one due to precipitate formation and growth.

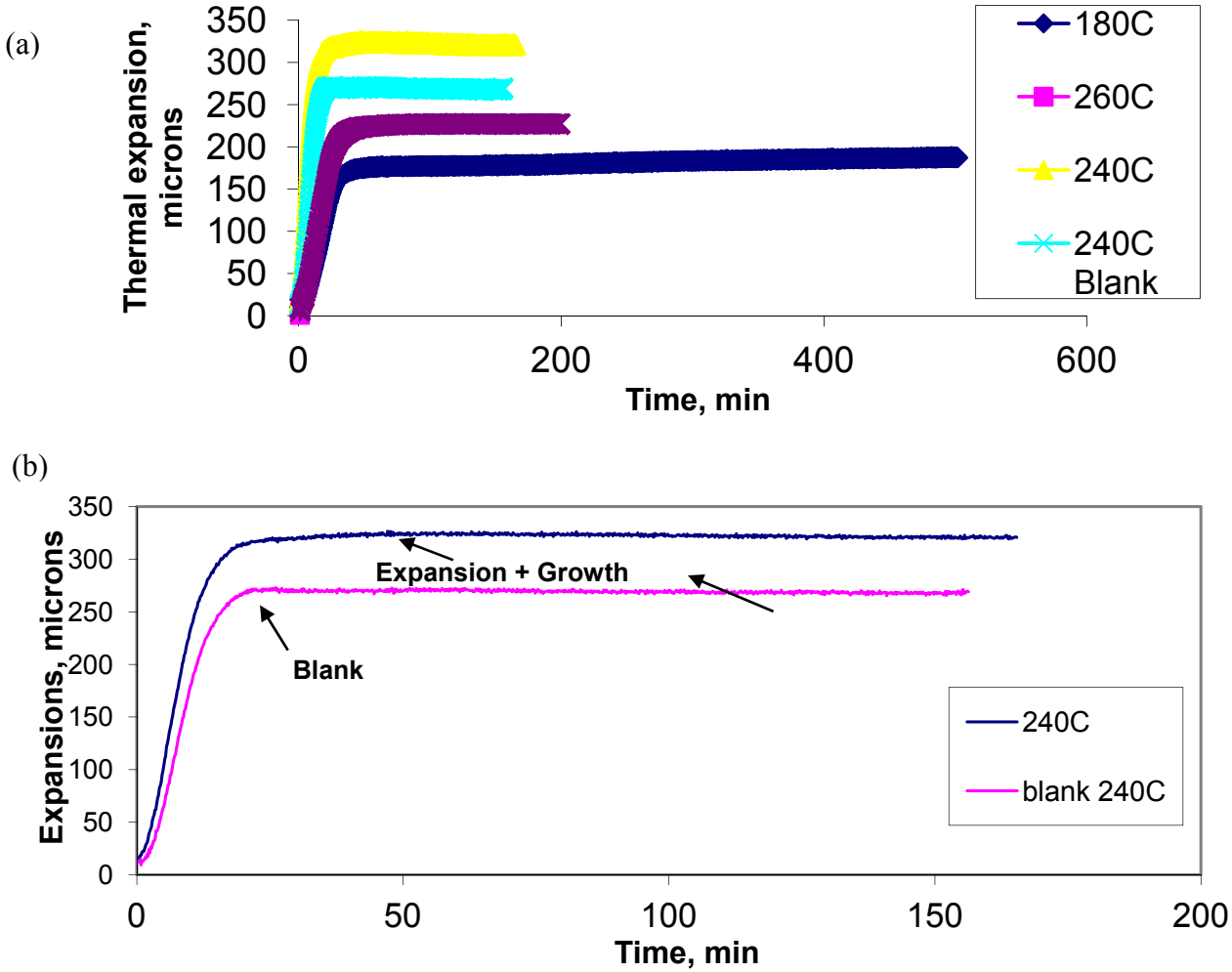

Figure 3. Dilatometric results showing (a) the magnitude of dimensional changes in the Al A319 at various temperatures and (b) contribution of precipitation to the dimensional alloy stability.

Also, notice from Figure 3b that there is a significant contribution of precipitate nucleation and growth to the alloy dimensional changes. Figure 4a shows the dimensional changes associated only with the precipitate transformation reactions occurring at 513 K (240 °C) as a function of time.

Figure 4b shows the rate at which these changes fall. Notice in particular that these changes tend to fade after 40–60 minutes.

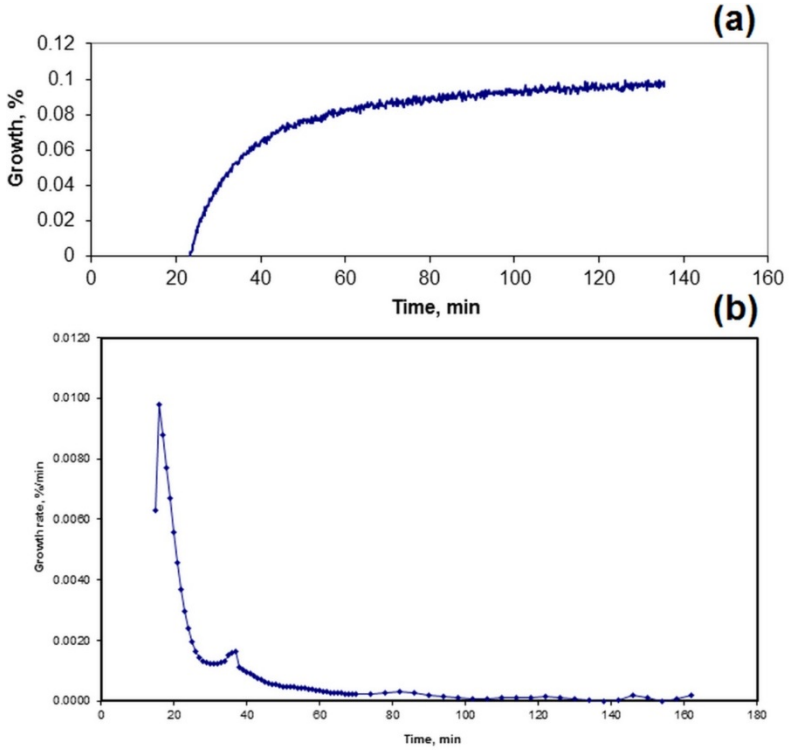

Figure 4. (a) Dimensional changes related to precipitation reactions at 513 K (240 °C) and (b) rate of dimensional changes with time in the Al A319 alloy.

3.2. Mechanical properties

As mentioned before, T7 heat treatments are often used in order to improve the alloy strength. In this work, tensile bars were tested at various times after exposure at 513 K (240 °C). The mechanical properties such as strength and ductility are plotted in Figure 5. From this figure it is evident that the T7 treatment improves the yield strength by approx. 100 MPa, reaching this maximum after approximately 2.5 hours. In contrast the alloy ductility drops from nearly 2% to barely 1%. From this graph peak aging conditions can be identified as corresponding to 2.5 hours. Beyond these times the alloy starts softening as manifested by a drop in strength and an increase in ductility.

Figure 6a shows the exhibited fracture surface exhibited by a tensile bar tested after ageing at 240 °C for 2.6 hours (T7 treatment). Notice from this micrograph the brittle nature of the fracture surface including the presence of relatively large "white" areas. These white regions are typical of Cu-rich regions which correspond to different intermetallic phases. In addition, Figure 6b shows a region near the fracture surface showing the cracking of brittle intermetallic phases.

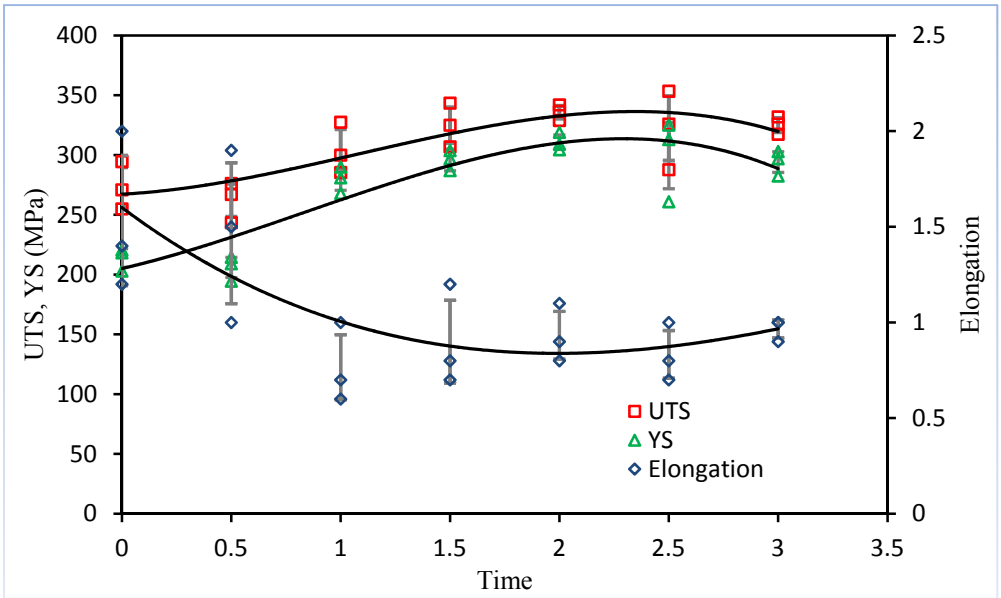

Figure 5. Mechanical properties exhibited by the Al A319 after ageing at 513 K (240 ^{o}C) for times of up to 3.0 hours.

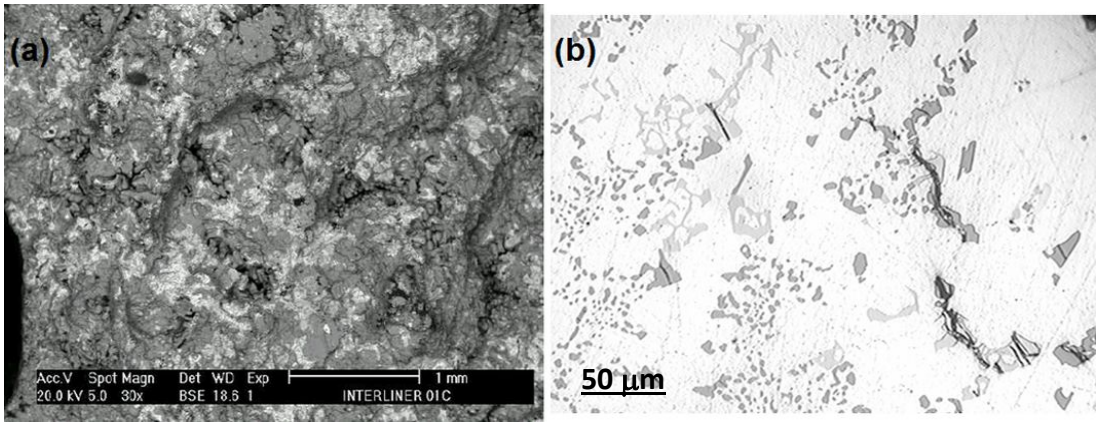

Figure 6. (a) Fracture surface showing the inherent brittle nature of the Al-A319 after T7 ageing at 240 °C for 2.6 h and (b) fractured intermetallic phases in a region adjacent to the fracture surface.

3.3. Transmission Electron microscopy

The alloys were investigated by TEM means where it was found that in the as cast condition a fine distribution of Si nanoparticles is present in the alloy matrix as shown in Figure 7.

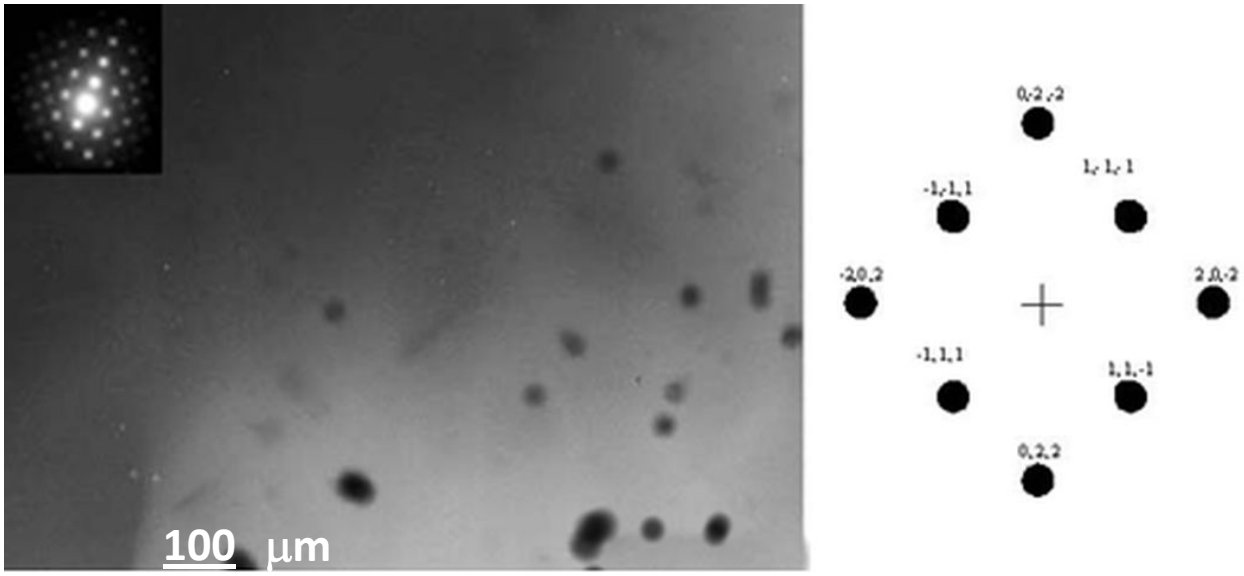

Figure 7. TEM micrograph and corresponding diffraction pattern of Si nanoparticles in the Al-A31 9 alloy in the as-cast condition.

After implementing the T4 treatment the Si nanoparticles seem to dissolve as there could not be found in the matrix. However, Cu-rich particles were identified in the matrix and they are shown in Figure 8. Notice that these particles are discretely distributed and they have nanometric sizes.

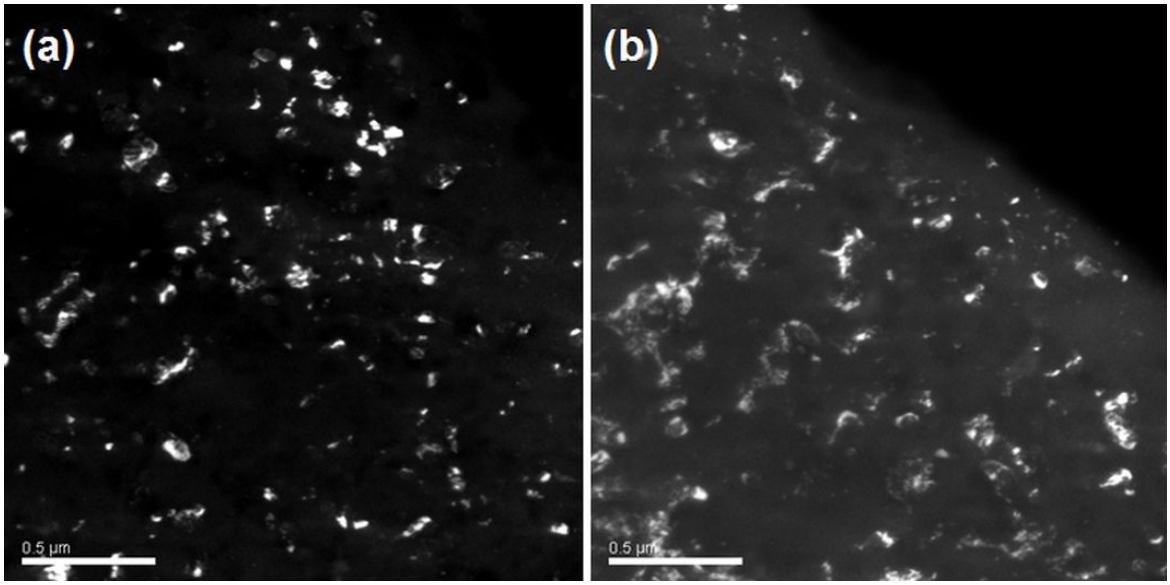

Figure 8. (a), (b) Dark Field TEM micrographs showing a distribution of Cu-rich (white color) particles in the Al-matrix.

The effect of T4 and T7 heat treatments was further examined by using high resolution TEM. Figure 10 shows the atom arrangement of the alloy matrix after the T4 heat treatment. From this figure, it is evident that no other phases precipitate in the Al alloy matrix.

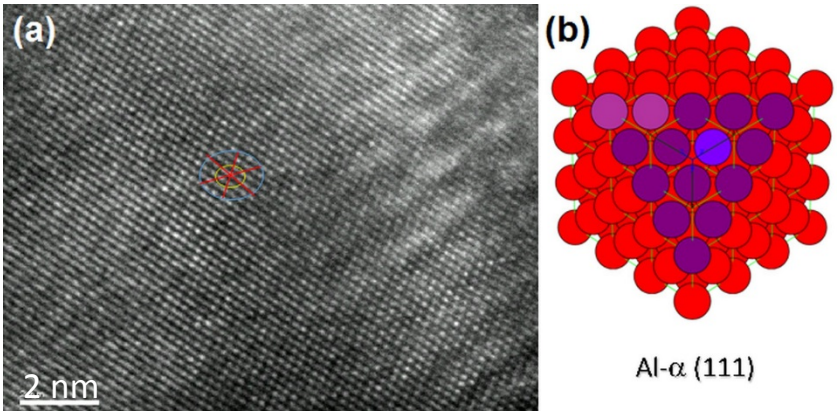

Figure 9. (a) High resolution TEM micrograph and (b) corresponding crystal structure model showing the lack of second phase precipitation in the Al-A319 alloy after solid solution T4 treatment.

Ageing for 1.5 hours at 513 K (240 °C) showed the formation of coherent θ' precipitates (see Figure 10). These precipitates are expected to contribute to dimensional changes due their low density or high specific volumes (see Table 2).

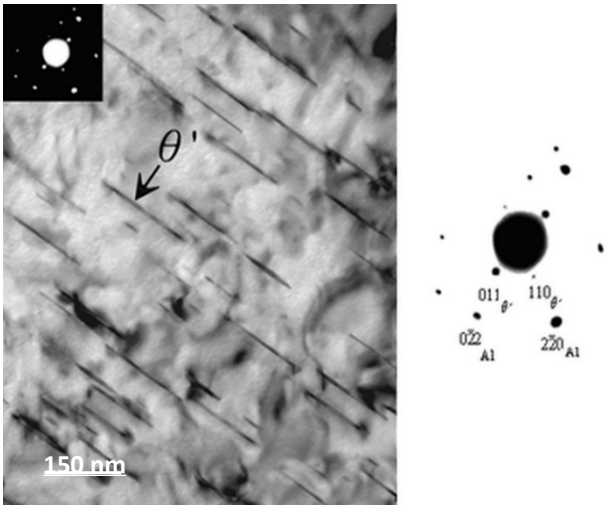

Figure 10. TEM micrograph and corresponding diffraction pattern of θ' precipitates in the A319 Al alloy after a T7 ageing at 513 K (240 °C) for 1.5 hours.

Under the T7-HT Cu-rich agglomerates again develop within the alloy. In this case, the Cu particles tend to coarsen and to become somewhat spherical (see Figure11) when compared with the ones in the T4 condition (Figure 8).

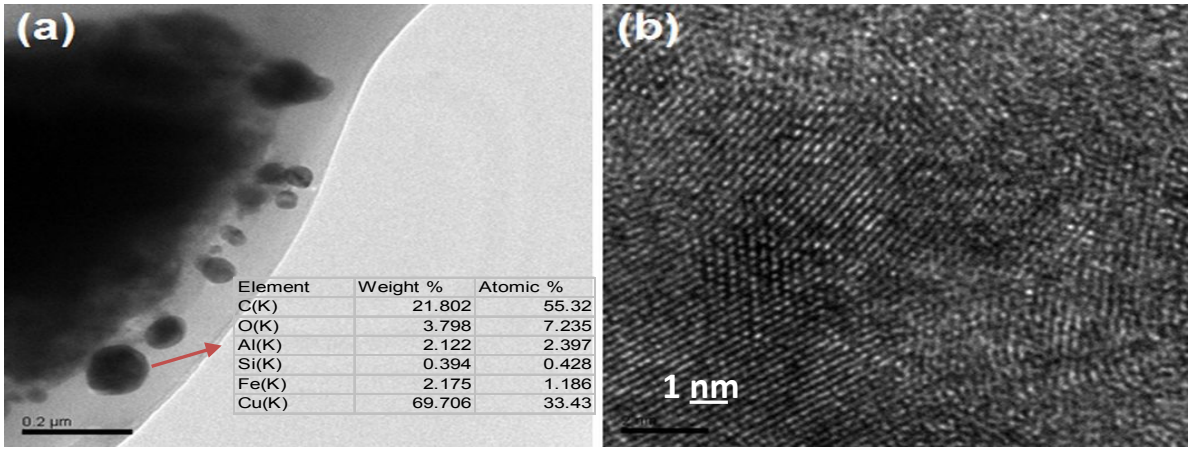

Figure 11. (a) TEM micrograph of Cu-rich spherical particles after T7 heat treatment (i. e. ageing at 513 K for 2.6 hours) in the Al A319 Al alloy and (b) High resolution TEM micrograph of the Al alloy matrix.

Moreover, the high resolution micrograph shows several crystals with random orientations and planar spacings. In turn, this indicates the development of other crystal structures within the matrix which are expected to be either θ' or θ precipitates as the alloy was aged for 3 hours at 513 K (240 °C). Thus, from this work it is found that Cu-rich particles or agglomerates are present in both the T4 and T7 conditions. Apparently, during the solubilization treatment not all of the Cu in the alloy is able to dissolve for the T4 conditions employed. Moreover, during ageing the Cu-rich particles seem to coarsen probably as a result of enough thermal energy and excess Cu which tends to accumulate as Cu-rich spherical particles.

4. Conclusion

The dimensional stability of an automotive Al-A319 was investigated after heat treating the alloy using a solution heat treatment (T4) at 753 k (480 °C) for 4.5 hours. Some of the T4 samples were subsequently aged at various temperatures and times (T7). Dilatometric testing indicated that the dimensional changes were due to alloy thermal expansion and the precipitation of secondary phases. This was followed by mechanical testing of T7 tensile bars after various ageing times. From these tests, it was found that the alloy strength consistently increased with ageing until a maximum value (peak aging condition) was found after 3 hours at 513 K (240 °C). Nevertheless, the alloy ductility dropped from 2% down to near 1%. An examination of the fracture surfaces indicated that the fracture path is rather brittle and it associated with Cu-rich intermetallics and regions. Microstructural evaluations by high resolution TEM showed that there is a distribution of Cu-rich particles in the matrix after T4 ageing. In turn, this indicates that not all of the Cu is dissolved during the T4 treatment. Moreover, during alloy ageing (T7) these Cu-rich regions apparently coarsen giving rise to spherical Cu-rich particles.

Conflict of Interest

The author declares no conflict of interest regarding this paper.

References

1. Rincon E, Lopez HF, Cisneros MM, et al. (2007) Effect of temperature on the tensile properties of an as-cast aluminum alloy A319. *J Mats Sci Eng A* 452–453: 682–687.
2. Rincon E, Lopez HF, Cisneros MM, et al. (2009) Temperature effects on the tensile properties of cast and heat treated aluminum alloy A319. *J Mats Sci Eng A* 519: 128–140.
3. Caceres CH, Svensson IL, Taylor JA (2002) Microstructural factors and the mechanical performance of al-Si-Mg and Al-Si Cu-Mg Casting alloys, Proceeds. 2nd Intl. Aluminum Casting Technology Symposium, Columbus Ohio. Eds. Tiryakioglu M and Campbell J. ASM Int., 49–57.
4. Tiryakioglu M, Campbell J, "Evaluating the structural quality of Cast Al-75 Si-Mg alloys by tensile deformation characteristics. Proceeds. 2nd Intl. Aluminum Casting Technology Symposium, Columbus Ohio, Eds. Tiryakioglu M and Campbell, ASM Int., 59–64.
5. Caceres CH, Svensson IL, Taylor JA (2003) Strength and ductility Behavior of Al-Si-Cu Mg casting alloys in T6 temper. *Int J Cast Metals Res* 15: 531–543.
6. Puncreobutr C, Lee PD, Kareh KM, et al. (2014) Influence of Fe-rich intermetallics on solidification defects in Al–Si–Cu alloys. *Acta Mater* 68: 42–51.
7. Aluminum Casting Technology (1997) in Metallography, Eds. American Foundry Society, 303–323
8. Aluminum, properties and physical metallurgy (1984) in precipitation heat treatment, Eds. ASM, 177–182.
9. Aluminum Casting Technology (1997) in Heat treatment and strengthening of aluminum castings, Eds. American Foundry Society, 287–302.
10. Brooks CR, Heat Treatment Structure and Properties of Nonferrous Alloys (1982) ASM, 95–114.

AIMS Press